Scientific Research and Essays Vol. 7(42), pp. 3584-3604, 31 October, 2012
Available online at http://www.academicjournals.org/SRE
DOI: 10.5897/SRE11.264
ISSN 1992-2248 © 2012 Academic Journals

Full Length Research Paper

Comparision of ant colony optimization and genetic algorithm models for identifying the relation between flow discharge and suspended sediment load (Gorgan River - Iran)

Omolbani Mohamad Reza Pour[1]*, Lee Teang Shui[2] and Amir Ahmad Dehghani[3]

[1]Zabol University, Zabol, Iran.
[2]Faculty of Engineering University Putra Malaysia, 43400 UPM Serdang, Selangor, Malaysia
[3]Gorgan University of Agricultural Sciences and Natural Resources, Gorgan, Iran.

Accepted 30 May, 2012

Correct estimation of sediment volume carried by a river is very important for many water resources projects. The prediction of river sediment load also constitutes an important issue in hydraulic and river engineering. Conceptual models based on artificial intelligence models, namely, ant colony optimization (ACO) and genetic algorithm (GA) are now being used more frequently to solve optimization problems. Hence, the main purpose of this study was to apply ACO and GA in order to identify the relation between stream flow discharge and sediment loads for Nodeh station at the Gorgan River in Iran. The training and testing data sets were chosen based on the K-fold method of cross validation to find the optimal classifier. Different input combinations of ACO and GA models (that is, ACO1 and GA1: the suspended sediment estimation based on current discharge; ACO2 and GA2: the estimation of suspended sediment based on current, one day of previous discharges; and ACO3 and GA3: the suspended sediment estimation based on current, one and two-day of previous discharges) were chosen based on similar meteorological requirements to those of the suspended sediment equations included in this study. The estimation of the ACO and GA models was also compared with the empirical model, such as the sediment rating curve (SRC) technique. The models were compared based on statistical criteria, namely; regression coefficient (R^2), Nash-Sutclif coefficient (CE) and root mean square error (RMSE). The results indicated that the ACO1 model provided better performance in estimating the suspended sediment loads as compared to the ACO models. Also, the GA2 model was more accurate than the GA1 and GA3 models. The findings in this study showed that the performance of the SRC model was more inferior the ACO and GA techniques when the inputs of the GA, ACO and rating curve models comprised only the current discharge. As seen from the results, the ACO1 model approximated that the corresponding observed suspended sediment values were better than the rating curve and GA2 techniques. However, for the peak flow discharge, the GA2 model could predict the suspended sediment better than the ACO2 and SRC models.

Key words: Suspended sediment, rating curve, ant colony optimization, genetic algorithm, Gorgan River, Iran.

INTRODUCTION

The volume and types of particles eroded and transported by the rivers exhibits great geographical and temporal variability. Predicting the sediment load of a river has long been a goal of engineers, hydrologists, sedimentologists, and many other earth scientists (Leopold et al., 1992). Accurate sediment load prediction is very important in planning, designing, operating and maintenance of water resources structures. Empirical relations, such as sediment rating curves, are often applied to determine the average relationship between discharge and suspended sediment loads. This type of models generally underestimates or overestimates the amount of sediment. Notably, direct measurement of sediment loads is very expensive to implement. Various models have been developed so far to identify the relation between discharge and sediment loads. Most of the models, based on the regression method, have some restrictive assumptions. Therefore, it is still necessary to develop an explicit model for the discharge-sediment relationship. Optimization models based on artificial intelligence models, namely, ant colony optimization (ACO) and genetic algorithm (GA) are now being used more frequently to solve optimization problems. In the early 1990s, ACO (Dorigo, 1992; Gambardella et al., 1999; Maniezzo, 1996) was introduced as a novel nature-inspired metaheuristic for the solution of hard combinatorial optimization (CO) problems. ACO belongs to the class of metaheuristics (Blum and Rol, 2003; Glover, 2002; Hoos et al., 2004), which are approximate algorithms used to obtain good enough solutions to hard problems in a reasonable quantity of computation time. Since then, ACO algorithms have been applied to different continuous and combinatorial problems, such as the travelling salesperson problem (TSP), the generalized assignment problem (GAP), the multiple knapsack problem (Leguizamon and Michalewicz, 1999), water distribution network design (Mariano and Morales, 1998), and the constraint satisfaction problem (Schoofs and Naudts, 2000). Abbaspour et al. (2001) used the ACO algorithm for estimating the unsaturated soil hydraulic parameters. Zecchin et al. (2003) compared the performance of original ant system with that of max-min ant system (MMAS), a modified version of the ant system proposed by Stutzle and Hoos (2001), for optimization of water distribution networks. Simpson et al. (2001) discussed the selection of parameters used in the ACO algorithm for pipe network optimization problems. More recently, Maier et al. (2003) compared the performance of the ACO algorithm with that of GA for the optimization of water distribution networks. Afshar (2005) proposed a new transition rule for ACO algorithms using elitist strategies and applied the method to pipe network optimization problems. The method was shown to overcome the premature convergence problem encountered by elitist ACO algorithms while improving the convergence characteristics of the algorithms as compared to alternative methods such as MMAS.

GA have been applied to numerous engineering problems such as management of water systems (Cai et al., 2001), design of water distribution networks (Savic and Walters, 1999), optimisation of sewer networks (Parker, 2000), calibration and improvement of urban drainage systems (Liong, 1995; James, 2002). In most applications, single objective GA were used such that only one criterion of optimisation was evaluated at a time and this is mainly due to the inadequate ability of single objective GA to deal with more than one objective. GA has been used frequently in the engineering problems in recent years. Sen and Öztopal (2001) used GA to predict precipitation occurrence. GA are also used in the optimization and operation of groundwater resources design uncertainties in the hydraulic conductivity and they also provide solution of more complex nonlinear problems when compared with traditional gradient based approaches (Espinoza et al., 2005; Hilton et al., 2005; Mahinthakumar et al., 2005). The sediment was predicted from discharge measurements using GA by Altunkaynak (2009).

Altunkaynaka and Wang (2010) proposed a new adaptive prediction approach termed Geno-Kalman filtering (GKF), combining GA and Kalman filtering techniques for accurate prediction of suspended sediment concentration (SSC). Their model is formed in three steps. Firstly, discharge and suspended sediment concentration are related by using dynamic linear model. Secondly, an optimum transition matrix relating these two state variables is obtained by Genetic Algorithms (GAs), and an optimum Kalman gain is calculated. Thirdly, Kalman filtering is used to predict the suspended sediment concentration from discharge measurement. They applied the proposed method to measurements at the Mississippi river basin in St. Louis, Missour.

Altunkaynaka (2010) developed some models for predicting suspended soild concentration based on 10 different scenarios for lake Okeechobee in Florida. Extensive data, including wind speed, flow velocity, flow direction and SSC, have been collected. They predicted the SSC by the Kriging interpolation technique.

Sen et al. (2004) proposed a new approach for sediment concentration prediction, and provided that there are measurements of discharge and sediment concentration. The basis of their methodology is a dynamic transitional model between successive time instances based on two variables, namely, discharge and sediment concentration measurements. The transition matrix elements are estimated from the measurements through a special form of the artificial neural networks as perceptrons. They achieved the sediment concentration predictions from discharge measurement through a perceptron Kalman filtering (PKF) technique.

The aim of this study is to obtain the relation between suspended sediment discharge and flow discharge for estimation of suspended sediment by using two optimization models that consist of ACO and GA and empirical model (SRC) for Nodeh station at Gorgan-river in Iran. Also, the result of each model was compared together in this study. In this study, the ACO (main aim of

*Corresponding author. E-mail: nrezaii2000@yahoo.com. Tel: 00601-73604770.

study) was developed because:

1) ACO imposes no continuity requirement on the objective function, and they can solve problems with discrete decision variables;
2) ACO usually does not get trapped to a local-optimal solution, and they can find a near-optimal solution with a high probability;
3) ACO generates several near-optimal solutions, and they can provide sufficient flexibility in decision making;
4) ACO have parallel processing potential, and they can generate faster solution in real (clock) time.

MATERIALS AND METHODS

The optimization and empirical models were used for estimating the suspended sediment in this investigation. The sediment rating curve through bias correction factor was used for the empirical models. The optimization models consisted of the ACO and GA models that were used for estimating the suspended sediment. GA was obtained from MATLAB toolbox, whereas ACO was developed for estimating the suspended sediment in C^{++}. For all the models, the daily flow discharge and the suspended sediment discharge measurements were used.

Empirical model or sediment rating curve (SRC)

In spite of very different methods for developing the rating curves, the most common method is the power function of the form $Y = aX^b$ which relates the suspended sediments concentrations to water discharge. Sediment rating curve expresses the sediment load, Q_s, at a cross-section from the river through its discharge, Q_w, as follow:

$$Q_s = aQ_w^b \tag{1}$$

Where Q_s is the suspended sediment discharge in (ton/day); Q_w is the stream discharge in (m^3/s); a, b are the coefficients that provide the best relationship between discharge and the sediment load. These parameters are generally obtained by least squares method. For a given set of Q_s and Q_w data, only one solution point (a and b) values are obtained. In this case, a and b coefficients are accepted as constant through all process. After log-transformation to the arithmetic domain and application of the Ferguson (1986) correction factor, the sediment load occurring at a specific discharge can be estimated using the following expression:

$$Q_s = C_f . a . Q_w^b \tag{2}$$

where C_f is the log-transformation bias correction factor

$$C_f = \exp(\frac{s^2}{2}) \tag{3}$$

where exp is the exponential function and s is the standard error of the regression equation. In the applications, Equation 2 is the sediment rating curve with bias correction factor was used for suspended sediment estimation.

Optimization models

The estimation of the suspended sediment depended only on the current discharge, because of the empirical models such as the sediment rating curve; in this study, flow discharges from the previous one- and two-days were also considered to improve the relationship between suspended sediment discharge and flow discharge, because the suspended sediment discharge has a relationship with discharges from the current, as well as from the previous one- and two-days.

The following equation shows the developed rating curve for the suspended sediment estimation:

$$Q_s = aQ_{w(t)}^b . Q_{w(t-1)}^c . Q_{w(t-2)}^d \tag{4}$$

where Q_s is the discharge of suspended sediments (ton/day); $Q_{w(t)}$ is the value of current discharge (m^3/s); $Q_{w(t-1)}$ is the value of previous one-day discharge (m^3/s); $Q_{w(t-2)}$ is the value of previous two-day discharge (m^3/s); a, b, c, and d are the determination coefficients.

The best unknown coefficients for a, b, c and d for the improved rating curve were obtained by minimizing the root mean square error (RMSE) between the observed suspended sediment discharge and the estimated suspended sediment discharge used (Equation 4). The training data was used to obtain the unknown parameters, and after that, obtained parameters were used for the test period. For minimizing the RMSE between the observed suspended sediment discharge and the estimated suspended sediment discharge using Equation 4, the developed ACO and GA approaches were used. Considering the use of the flow discharge for the improved rating curves by GA and ACO, three sub-models were being created for each of them. If the data of the current day discharge were used for estimating the suspended sediment in Equation 4, the corresponding models of ACO and GA were called ACO1 and GA1; whereas, if the data of the current and one-day previous discharges were used, they were then called ACO2 and GA2. When the current, one and two-day previous discharges were used, the ACO and GA were called ACO3 and GA3. Table 1 summarises the parameters that were used for each model.

GA

This global optimisation (GA) procedure is based on the Darwinian principle of survival of the fittest. Applied to a biological community, it is the principle by which chances of survival of an entire community within a particular environment are increased by discarding inferior members and replacing them by superior offspring. The probability of survival of the community increases as it develops characteristics required to extract maximum benefit from resources within its new environment. This stage is reached over a period spanning many generations and is the result of improving genetic combinations of individual members through reproduction of the fittest. Theoretically, a near optimal solution could perhaps be obtained even within the initial population, if it were possible to formulate a parameter set by taking the best value of each parameter across population members. Given a sufficiently large population, every parameter would assume values evenly

Table 1. Discharge identity parameter used for corresponding model.

Variety of conceptual models	Current discharge ($Q_{w(t)}$)	Current discharge and one day previous discharge ($Q_{w(t-1)}$)	Current discharge, one and two day previous discharge ($Q_{w(t-2)}$)
ACO1	*	-	-
ACO2	*	*	-
ACO3	*	*	*
GA1	*	-	-
GA2	*	*	-
GA3	*	*	*
SRC	*	-	-

distributed over its parameter range. Careful formulation of the genetic plan is required to produce balance between exploitation of the entire search space and exploration of the interesting regions of attraction.

In this part of this research, genetic algorithm improved the sediment rating curve for one and two days before the current discharge. GA with the training data minimized the RMSE between the observed suspended sediment discharge and the simulated suspended sediment discharge for obtaining the coefficient of Equation 4. The best coefficient was found when the lowest RMSE was obtained and the GA stopped. The calculated coefficient through GA was then used for the test period. The following is the first description of the objective function for genetic algorithm. In this study, the objective function was to find a factor set γ that minimized the general function by using GA:

$$g(\gamma)=\sum_{i=1}^{l}\sqrt{(Q_m-Q_o)^2} \quad (5)$$

Where g is the objective function; γ is the vector of input factor; l is the number of observed variables; Q_o is the measured value of suspended sediment discharge of the ith variable (ton/day); and Q_m is the simulated suspended sediment discharge from Equation 4 (ton/day).

Careful formulation of the genetic plan was required to produce the balance between the exploitation of the entire search space and the exploration of the interesting regions of attraction. For this research, all the functions were examined together for finding the best function. GA may achieve this best combination via its genetic plan, which is a procedure consisting of the following operators:

1) Selection, which randomly chooses a sub-set of individuals for mating from among the whole population;
2) Replacement, which is the mechanism of incorporating into the original population the offspring resulting from mating at the expense of inferior individuals;
3) Crossover, which is the method of swapping genes during mating of selected individuals to produce offspring;
4) Mutation, which randomly alters selected genes in chromosomes and which will be discussed subsequently.

These steps are repeated until a certain error percentage is achieved between two final successive solutions. In the first step of the algorithm, initial population is constituted through the chromosomes that are selected randomly. The number of chromosomes in the population is decided by the user. This population changes by certain rules in order to optimize the target function. Each chromosome should be evaluated by considering their objective function to find the optimum solution. During the evolution of the solution population, some chromosomes depart from the process while stronger ones remain in the updated population. In order to constitute the new generation, chromosomes that provide the most suitable conditions for objective function are selected by using Roulette wheel. This wheel is partitioned into sections of which the widths are determined according to the objective function. So, the chromosomes which have best objective function value have a more chance to be selected as members for the next generation. The new generation is evolved from the current generation by applying some genetic operators such as cross-over and mutation. These operations are repeated until the objective function is achieved. The number of iterations required to obtain the optimal coefficient values depend on the initial population. If the initial population is close to solution point, the algorithm would reach the solution with less iteration. Since GA produce many solution points, they put forward the relationship between discharge and sediment by forming more than one curve using a and b parameters in Equation 4. The flow chart of the genetic algorithm used in this study is as shown in Figure 1.

ACO

ACO is now being used more frequently to solve optimization problems other than those for which they were originally developed. However, the application of ACO to water resources problems is rather recent. In this part of the research, ACO can improve the sediment rating curve for one and two-day discharges before the current discharge. ACO with the training data (from sample data) minimized the RMSE between the observed suspended sediment discharge and the simulated suspended sediment discharge in order to obtain the coefficient of Equation 4. ACO continues until the lowest RMSE is obtained. The best coefficient was found when the lowest RMSE was obtained, after which ACO was stopped. The calculated coefficient was used for the test period (from sample data).

Application of ACO to estimated suspended sediment: During the past several decades, considerable advances have been made in the mathematical description of water flow and suspended sediment transport. A large number of models are now available for predicting the subsurface flow and suspended sediment. Still, effective application of such models to practical field problems suffers from the lack of knowledge of model parameters and their uncertainties.

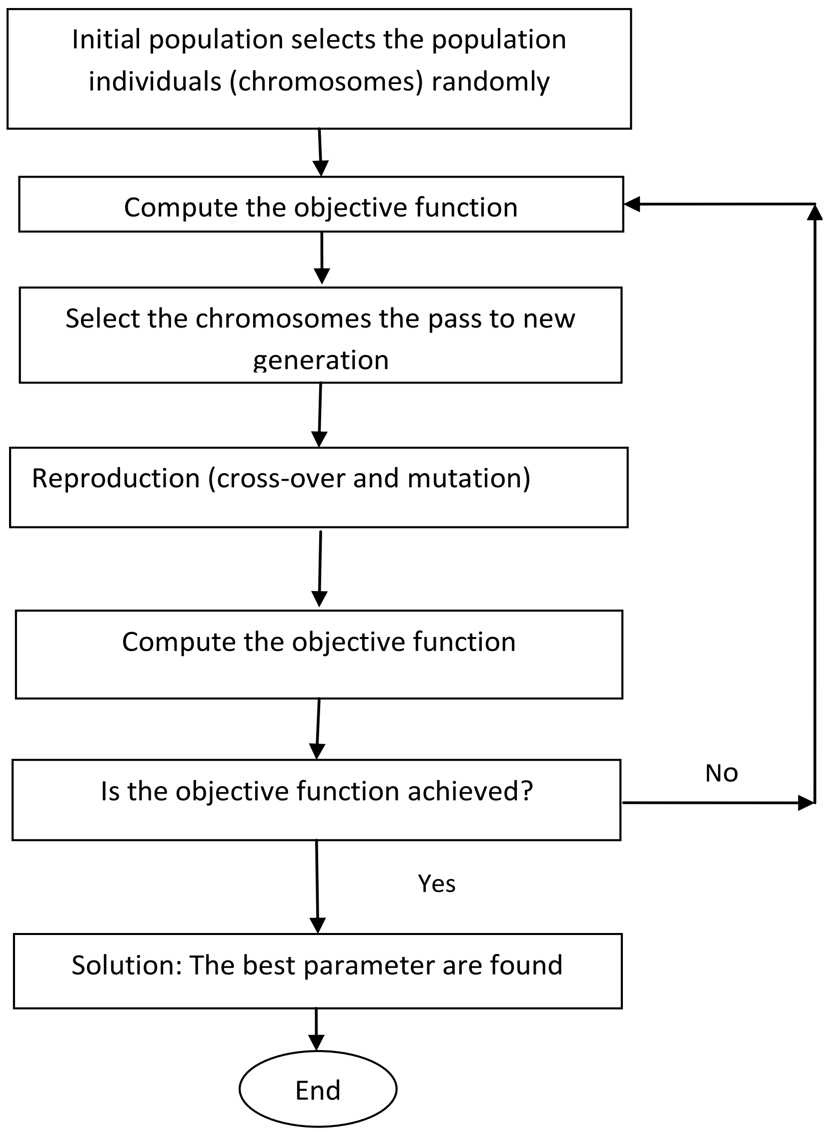

Figure 1. Flow chart for GA.

In order to deal with the issue of model factor identification, inverse modelling (IM) from ant system (AS) algorithm provides that constituted estimation of input factors from readily measurable model output variables. Input factors are obtained by minimizing an objective function describing the difference between the measured and simulated data (Abbaspour et al., 2001).

The first in this part of the study was to describe the objective function. In this study, the objective function was the same with the objective earlier explained in the part of GA. As mentioned previously, the objective function is to find a factor set γ that minimizes the general function repeated here for convenience:

$$g(\gamma) = \sum_{i=1}^{l} \sqrt{(Q_m - Q_o)^2}$$

In the ACO algorithm, a colony of artificial ants contributes in finding good solutions to discrete optimization problems. Application of the ACO algorithm to arbitrary combinatorial optimization problem requires that the problem can be projected on a graph (Dorigo, 1996). Consider a graph G = (J, γ, U), in which J = { $j_1, j_2,.... j_n$ } is the set of decision points at which some decisions are to be made; γ = {γ_{il}} is the set of options; L = 1,2,...,l, at each of the determination points; i = 1,2,...,n; and finally U = {u_{il}} is the set of costs associated with options γ = {γ_{il}}.

The main concept behind the algorithm can be summarized in the following steps:

1) Depict each unknown factor by an interval based on the available information for the imaginary factor γ, as shown in Figure 2;
2) Discrete each interval into a number of level, and let the middle of each layer represent that layer;
3) Run the simulation model of the selected subset of all the possible factor combinations (a loop);
4) Grade each layer on the basis of the smallness of the value of

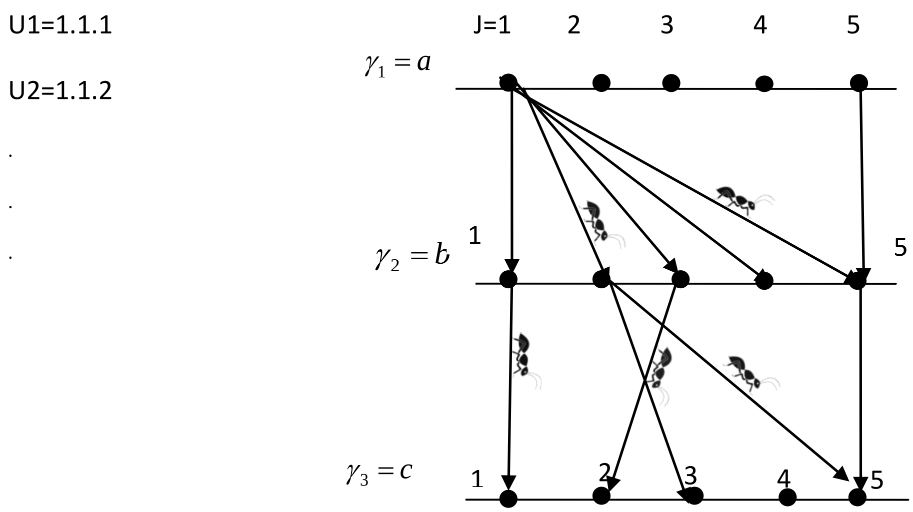

Figure 2. Schematically scheme of nerve tract structure.

the objective function received higher grade;
5) Remove from the ends of the factor intervals the level with small or no grade, thereby, decreasing the initial range of factor uncertainty, and finally;
6) Repeat the process until a desired stopping rule is reached.

In the algorithm, each layer, which is initially set to a grade of zero, receives a grade of 1 if the numerical quantity of the objective function g, for that layer satisfies the condition ($g \le g_{cr}$) , where g_{cr} is the user defined numerical quantity (Abbaspour et al., 2001).

Explication of the ACO: The ACO problem can be described as follows: let $g(\gamma)D \rightarrow R$, as given by Equation 6 be a continuous and bounded function, and γ be a b-dimensional state vector. The objective is to find the state vector γ that minimizes g (γ). Without the loss of generality, D can be taken as the hyper parallelepiped:

$$D=\left\{\gamma_i \middle| \gamma_i^- \le \gamma_i \le \gamma_i^+; i=1,2,...,b\right\} \tag{6}$$

where γ_i^- and γ_i^+ denote, respectively, the lower and upper bounds of factor γ_i. This is done by separating the interval $[\ \gamma_i^-, \gamma_i^+\ ]$ of each factor γ_i into a number, say w_i, of the level (Abbaspour et al., 2001).

Note that in this study, $\gamma_1 = a$, $\gamma_2 = b$, $\gamma_3 = c$ and $\gamma_4 = d$. If each layer is represented by the numerical quantity at the middle of the layer, then there will be W = $w_1.w_2...w_b$ switch or possible nerve tracts through the space of the input factors. The aforementioned decretive scheme for the three factors is schematically shown in Figure 2.

While having more levels would speed up the convergence of the ACO problem, this advantage should be balanced against the speed of the simulation programme, which rapidly increases as the number of calls to a simulation programme rapidly increases as the number of level increases. To limit the number of function calls, one could select only a random subset of M or N and invoke parallel processing. Based on Abbaspour experience so far, $N \ge 0.1M$ generally leads to optimum solutions.

Attribute tasks to ant agentive role: The total number of ant *m* in the colony is chosen because any ant must follow one nerve tract. Acting like an agentive role, each ant has the following tasks:
1) Selecting a nerve tract from the nerve tract list and remembering the numerical quantities of the factor level along its nerve tract;
2) Passing the factor numerical quantities to a simulation programme at the end of the nerve tract;
3) Calculating the numerical quantity of the objective function for its nerve tract, and
4) Placing a certain pheromone in the case of real ants on the basis of the numerical quantity of the objective function.

Once all ants complete the aforementioned circuit, one ant cycle or one loop is completed (Abbaspour et al., 2001).

Counting the trail and grading factor level: Pheromone trails play an important function in the foraging behaviour of the real ant colonies. While walking from food sources to the nest and vice versa, ants stick on the ground a substance called pheromone, forming in this way a pheromone trail. Ants can smell pheromone and, when choosing their way, they tend to choose, in probability, routes marked by strong pheromone densities (Abbaspour et al., 2001).

The pheromone trail acts as a form of indirect social relation called stigmergy helping the ants to find their way back to the food source or the nest. In ACO, pheromone trails are the only social relation channel among the ants and play a major role in the utilization of collective knowledge of the colony (Abbaspour et al., 2001).

Let $\tau_u(1)$ be the intensity of pheromone on nerve tract u (u = 1,…N) and cycle 1. Ants must place the same quantity of pheromone on the layers that they follow. In the Travelling Salesman Problem (TSP), the trail intensity is defined as a function of the length of a route. In this problem, we used the numerical quantity of the objective function of a nerve tract to ascribe the trail.

$$\tau_u(I)=\begin{cases}\exp(4.6(\frac{g_u-g_{cr}}{g_{\min}-g_{cr}})),....g_u \le g_{cr}, \\ 0..................................g_{u\ge g_{cr}}\end{cases} \quad (7)$$

where g_u is the numerical quantity of the objective function for the u[th] nerve tract, g_{cr} (will be defined later) is a critical numerical quantity and $g_{\min}$ is the minimum numerical quantity of the objective function for a cycle (Abbaspour et al., 2001).

The aforementioned Equation (7) posits that the nerve tracts with numerical quantities of the objective function larger than g_{cr} receive no pheromone, while below g_{cr}, the intensity of trail is exponentially larger for smaller numerical quantities of the objective function. At $g_{\min}$, $\tau_u(1)$ is a set equals to an arbitrary numerical quantity of 100 (this numerical quantity would be equivalent to Q in the TSP, which also incidentally equals 100) (Abbaspour et al., 2001).

In order to determine how to update the factor, we defined the term grade S_i for each layer counted by the following expression similar to the transition probability of the TSP problem.

$$\underset{g_{cr}=T}{S_{ij}}=\frac{(\Phi_{ij})^A(\delta_{ij})^N}{\sum_i\sum_j(\Phi_{ij})^A(\delta_{ij})^N} \quad (8)$$

where the numerical quantity of A = 1, and count N and T by using,

$$N=C_N\frac{\delta_{ij}}{\mu_{ij}} \quad (9)$$

$$g_{cr}=g_{\min}+c_T\frac{\delta_g}{\mu_g} \quad (10)$$

where δ_{ij},μ_{ij} are respectively the standard deviation and mean of trail of the γ_{ij} level (Abbaspour et al., 2001). δ_g,μ_g are respectively, the standard deviation and mean of the objective function for a loop, and C_T and C_N are constant that were determined to be about 0.8 and 0.5, respectively. The factor A, N and T in Equation 8 control the relative importance of the trail intensity versus sensitivity. Note that any single layer γ_{ij} may be the crossroad of many ant nerve tracts. The trail share of each layer γ_{ij} form each nerve tract, and can be summed to yield φ_{ij} as:

$$\varphi_{ij}(1)=\sum_{u\varepsilon\Xi crossin\,gpathways}\tau_u(1) \quad (11)$$

where crossing nerve tracts are all the nerve tracts that cross layer γ_{ij} (Abbaspour et al., 2001). The work Abbaspour (2001) has more information about this algorithm.

Updating factors and stopping rules: The counted trail for each nerve tract is used to grade a nerve tract. The low grading nerve tracts will vanish and new nerve tracts will evolve around high grading routes (Abbaspour et al., 2001).

Once the grading is completed, the factors are updated by decimating the level with small grades from both ends of the intervals. This results in factors with narrower ranges. Note that, if the high grading level falls on either end of the factor intervals, the factors could be extended in that direction. The system is subsequently reinitialized, with the updated factors and the process repeated. This loop continues until a stopping rule is satisfied. This may occur when: (1) a desired numerical quantity of the objective function is reached, and (2) no changes in the numerical quantity of the objective function are obtained in the consecutive loops. Figure 3 shows the flow chart for ACO.

Study area and data

The Gorgan River watershed is located in the southeast of the Caspian Sea between 54°,02' - 56°,16' east longitude and 36°,34' - 37°,47' north latitude. The Gorgan River originates from the high lands of the Alborz mountain chains at the eastern part of the watershed. After passing through the city of Gonbad Kavous, it enters into Voshmgir Dam and finally joins the Caspian Sea. The watershed of Gorgan River spreads over an area of 13170 km^2 approximately, 7838 km^2 (60%) of which accounts for the watershed highlands, and the remainder includes foothills and plains. Nearly 8500 km^2 of the watershed is covered by the Basin of Gorgan River, which extends to the Voshmgir Dam. Figure 4 shows the location of Gorgan River basin and Voshmgir Dam.

In this study, the mean river flow discharge and the suspended sediment concentration data at Nodeh station on the Gorgan River in Iran were used. These data, gathered from the Water Resource in Golestan province from 1978 until 2008, were divided into two partitions, that is, one for training and the other for testing. It was important to separate the data sets into two separate sets, that is, one to be used for training and the other for testing the results obtained from the training. K-fold cross validation was used in the field of machine learning to determine how accurately a learning algorithm would be able to predict data that it was not trained on.

Efficiency criteria

Here, the efficiency criteria used in this study are presented and evaluated. These are the three criteria: coefficient of determination, Nash-Sutcliffe efficiency, and RSME present in the model simulation.

Coefficient of determination (R^2)

The coefficient of determination R^2 is defined as the squared value of the coefficient of correlation according to Bravais-Pearson. It is calculated as:

$$R^2=\left(\frac{\sum_{i=1}^{n}(O_i-\overline{O})(P_i-\overline{P})}{\sqrt{\sum_{i=1}^{n}(O_i-\overline{O})^2}\sqrt{\sum_{i=1}^{n}(P_i-\overline{P})^2}}\right)^2 \quad (12)$$

With O observed and P predicted values. R^2 can also be expressed

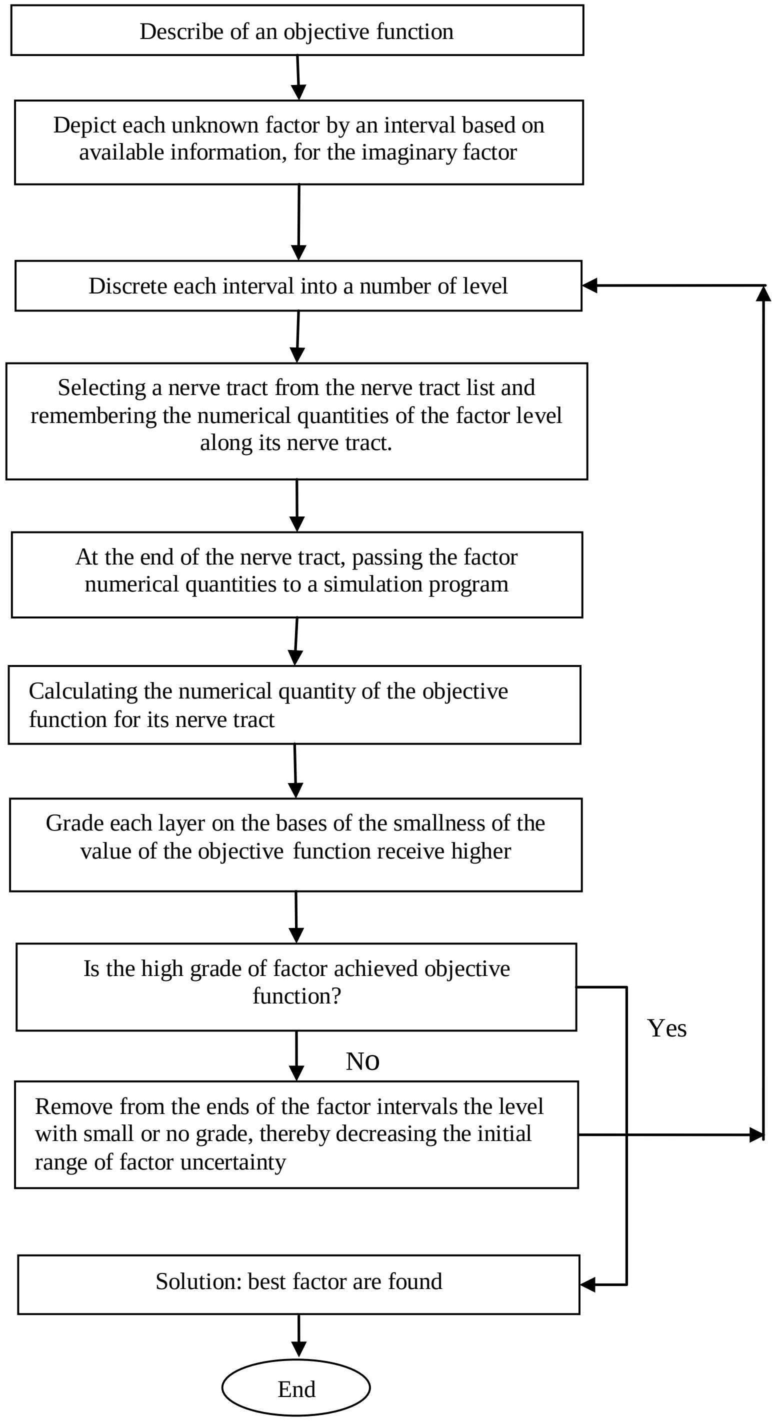

Figure 3. Ant colony optimization flowchart.

as the squared ratio between the covariance and the multiplied standard deviations of the observed and predicted values. Therefore, it estimates the combined dispersion against the single dispersion of the observed and predicted series. The range of R^2 lies between 0 and 1 which describes how much of the observed dispersion is explained by the prediction. A value of zero means no correlation at all, whereas a value of 1 means that the dispersion of the prediction is equal to that of the observation. The fact that only the dispersion is quantified is one of the major drawbacks of R^2 if it is considered alone. A model which systematically over- or under predicts all the time will still result in good R^2 values close to 1.0 even if all predictions were wrong.

Nash-Sutcliffe efficiency

The coefficient of efficiency (CE) proposed by Nash and Sutcliffe (1970) is defined as one minus the sum of the absolute squared

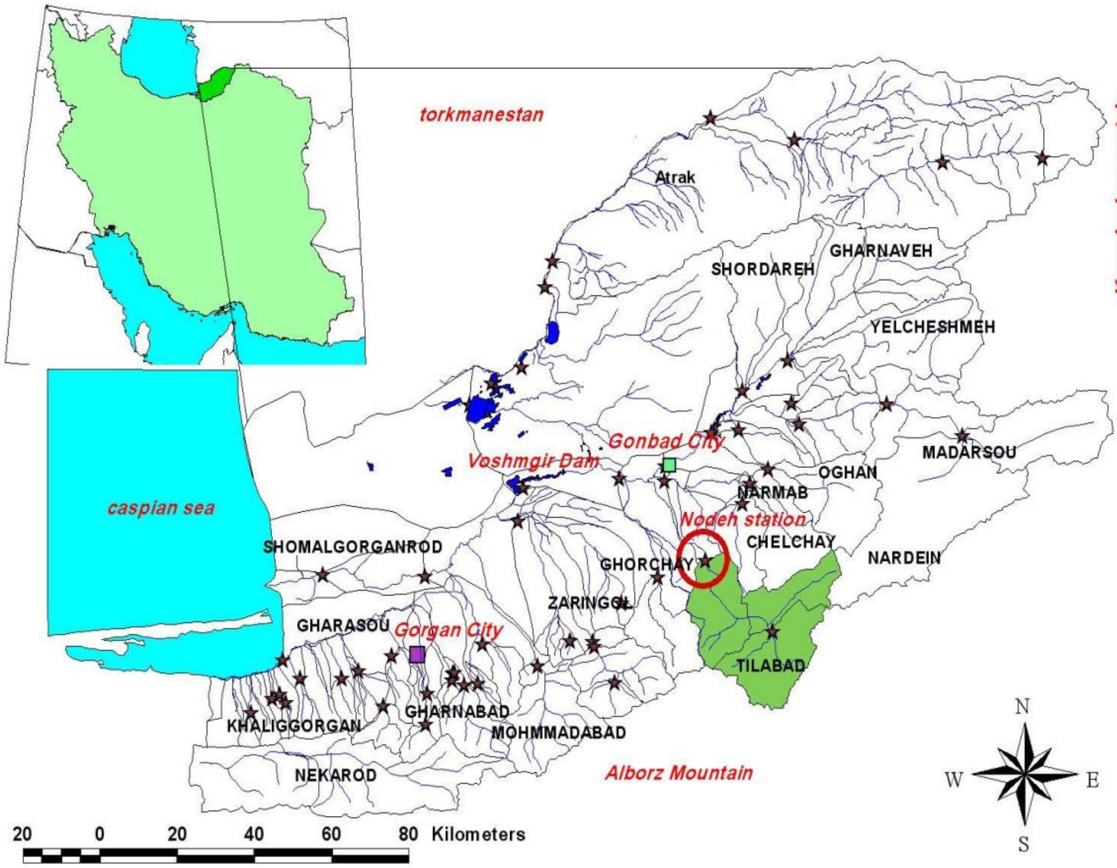

Figure 4. Location of the Gorgan River Basin and Nodeh station.

differences between the predicted and observed values normalized by the variance of the observed values during the period under investigation. It is calculated as:

$$CE = 1 - \frac{\frac{1}{N}\Sigma_1^N (O-P)^2}{\frac{1}{N}\Sigma_1^N (O-\bar{O})^2} \tag{13}$$

where CE is the coefficient of efficiency, N is the number of data points, O is observed value and P is predicted value.

Nash–Sutcliffe efficiencies can range from −∞ to 1. An efficiency of 1 (CE = 1) corresponds to a perfect match of model discharge to the observed data. An efficiency of 0 (CE = 0) indicates that the model predictions are as accurate as the mean of the observed data, whereas an efficiency less than zero (CE < 0) occurs when the observed mean is a better predictor than the model or, in other words, when the residual variance, is larger than the data variance.

RMSE

$$RMSE = \sqrt{\frac{1}{N}\sum_{i=1}^{n}(O-P)^2} \tag{14}$$

where, RMSE is the root mean square error, N is the number of data points, O is observed value and P is predicted value.

RESULTS

The scatter plots of the Nodeh station data for determining the relationship between the discharge and sediment data were used, as shown in Figure 5. It can be seen that there was a non-linear and scattered relationship between the discharge and sediment data for this station. The daily statistical parameters of the stream flow and sediment data were x_{mean}, $X_{\max}$ and $X_{\min}$ denoting the mean, maximum and minimum of data, respectively. The daily statistical parameters of the stream flow and sediment data are given in Table 2.

The results of each model are shown in the subsequently. Considering the presentation of results from the each month, it took more time and attention than only the results of April declared.

Sediment rating curve

As for the SRC model, the daily discharge and sedimentation data of 30 years were used for the monthly method. Prior to application, the SRC data were divided into two parts, namely, calibration and validation. The training data was used to find the model parameters

Table 2. The daily statistical parameters for monthly flow discharge (m^3/s) and suspended sediment (ton/day).

Test period	Data type	Xmin	Xmax	Xmean
April	Flow	1.43	10.66	4.95
	Sediment	27.46	1845.64	450.81
May	Flow	0.47	6.94	2.81
	Sediment	2.00	574.16	93.43
June	Flow	0.02	7.05	1.83
	Sediment	0.02	493.79	53.20
July	Flow	0.06	2.85	0.93
	Sediment	0.07	38.10	10.35
August	Flow	0.40	3.28	1.21
	Sediment	0.07	402.79	32.92
September	Flow	0.48	3.32	1.54
	Sediment	1.67	292.97	33.36
October	Flow	1.30	3.42	2.23
	Sediment	8.98	113.59	34.07
November	Flow	1.12	2.93	1.98
	Sediment	4.08	68.94	23.68
December	Flow	0.77	3.45	1.92
	Sediment	1.32	78.59	21.26
January	Flow	0.89	7.30	2.13
	Sediment	0.65	859.88	55.19
February	Flow	1.02	5.61	2.29
	Sediment	4.40	211.88	45.46
March	Flow	1.62	12.88	3.72
	Sediment	8.56	2511.29	240.13

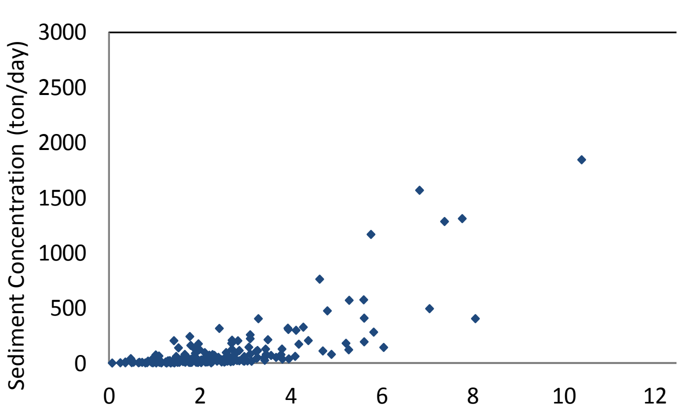

Figure 5. Suspended sediment load–discharge scatter diagram for all data for the Nodeh station.

(coefficients of a and b), while the rest of the data was employed for validation of the model. On the other hand, in Figure 6, the scatter plot for the observed and estimated suspended sediments for April was drawn by the SRC model. Meanwhile, Figure 7 shows the scatter plot of the discharge against the observed suspended sediment load and the estimated suspended sediments by SRC, whereas Table 3 displays the RMSE, coefficient of determination (R^2) and Nash's Efficiency (CE) values.

GA

Several input combinations are checked using GA to estimate suspended sediment load for the Nodeh station. The RMSE, coefficient of determination (R^2), Nash-Sutcliffe

Table 3. The RMSE (ton/day), coefficient of correlation and determination coefficient of SRC models for test period.

Test period	SRC				
	RMSE	R^2	a	b	CE
October	5.539	0.525	11.03	1.149	0.54
November	4.892	0.234	1.91	2.678	-5.47
December	4.540	0.610	4.359	1.595	-1.89
January	69.870	0.801	7.286	1.56	0.25
February	8.521	0.065	13.56	1.271	-6.05
March	23.328	0.238	8.904	2.118	0.05
April	109.446	0.656	3.061	2.799	0.39
May	34.548	0.168	12.01	1.407	0.26
June	27.241	0.408	13.62	1.395	-0.62
July	0.839	0.389	10.63	1.124	0.57
August	3.100	0.597	6.624	2.768	-1.2
September	3.942	0.325	9.57	1.436	0.42

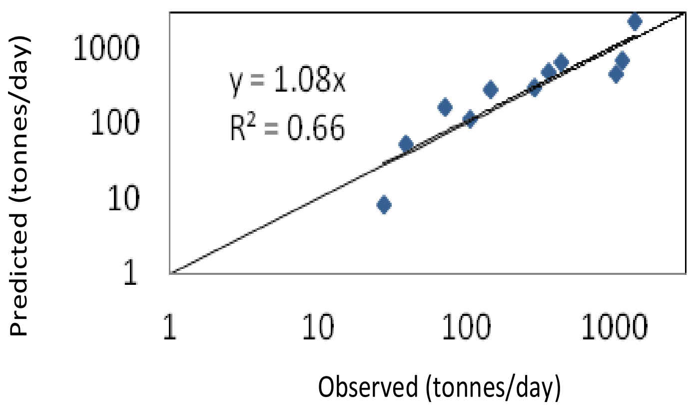

Figure 6. Scatter plot for observed and predicted suspended sediment for test period for various SRC for April.

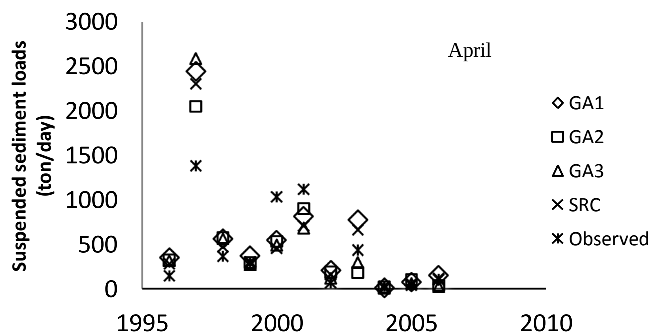

Figure 8. The scatter plot of the discharge against the observed suspended sediment load and the estimated suspended sediment by GA models of Nodeh station during test period in April.

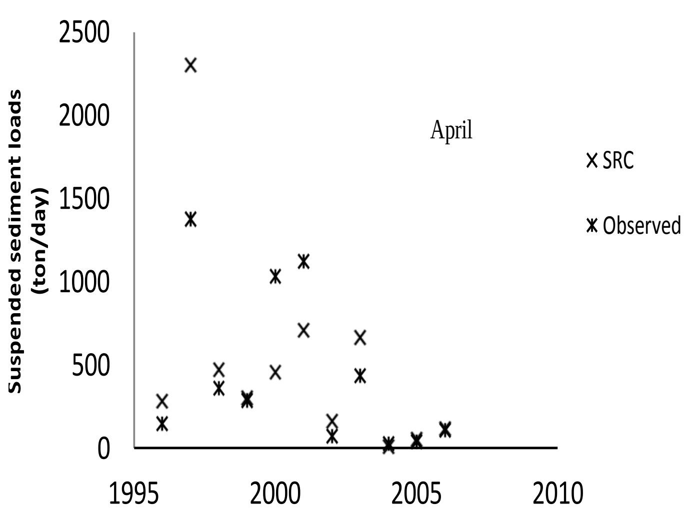

Figure 7. The scatter plot of the discharge against the observed suspended sediment load and the estimated suspended sediment by SRC of Nodeh station during test period in April.

efficiency (CE) and coefficients that provide the best relationship between discharge and the sediment load of GA models in test period are shown in Table 4. For GA optimization, constant parameters, sets of a, b, c and d parameters were obtained from training data. The scatter plot of the discharge against the observed suspended sediment load and the estimated suspended sediment by GA models of April is as shown in Figure 8. Also in Figure 9, the scatter plot for the observed and estimated suspended sediment for April is drawn by parameters found as a result of GA optimization.

ACO

For the Nodeh station, the RMSE, coefficient of determination (R^2), Nash-Sutcliffe efficiency (CE) and coefficients that provide the best relationship between discharge and the sediment load of ACO models in test period are given in Table 5. For ACO optimization, parameters, sets of a, b, c and d were obtained from

Table 4. The RMSE (ton/day), coefficient of correlation and determination coefficient of variety of GA and SRC models for test period.

Test period	RMSE	R^2	a	b	c	d	CE
GA1							
October	117.835	0.67	5.306	2.591	-	-	0.30
November	53.291	0.398	4.254	2.68	-	-	-0.76
December	21.383	0.854	5.892	2.296	-	-	-0.17
January	1.282	0.482	9.289	2.25	-	-	0.42
February	8.177	0.61	11.366	3.008	-	-	-14.4
March	4.111	0.356	6.498	2.389	-	-	0.13
April	5.124	0.349	15.917	0.963	-	-	-0.16
May	4.248	0.357	5.08	1.99	-	-	-3.88
June	4.013	0.606	6.322	1.728	-	-	-0.48
July	71.528	0.908	3.733	1.84	-	-	0.21
August	8.404	0.227	4.751	2.12	-	-	-1.78
September	23.447	0.254	7.262	2.288	-	-	0.00
GA2							
October	86.926	0.736	1.906	1.126	2.002	-	0.62
November	42.998	0.347	5.633	2.801	-0.669	-	-0.15
December	19.788	0.8	8.927	2.066	-0.016	-	0.65
January	1.6784	0.595	3.701	3.531	0.395	-	-0.80
February	9.899	0.619	2.186	4.132	1.317	-	-21.6
March	2.599	0.473	4.565	4.876	-2.233	-	0.29
April	4.557	0.599	12.179	1.009	0.209	-	0.09
May	4.171	0.054	6.324	1.38	0.317	-	0.39
June	3.947	0.593	6.244	2.34	-0.574	-	-0.56
July	74.174	0.91	2.044	1.709	0.503	-	0.15
August	7.729	0.295	4.948	0.583	1.116	-	-0.84
September	27.678	0.259	2.35	2.652	0.197	-	-0.20
GA3							
October	130.203	0.632	0.472	1.665	1.087	1.107	0.14
November	37.550	0.333	6.135	2.806	1.558	-2.276	0.12
December	26.083	0.660	6.558	2.304	0.077	-0.278	0.08
January	1.721	0.169	1.51	2.477	2.454	0.757	-3.20
February	9.569	0.628	3.872	3.979	0.023	0.728	-20.1
March	3.015	0.176	4.03	5.801	-0.839	-2.51	0.03
April	5.120	0.575	5.566	1.894	-0.839	0.95	0.21
May	4.620	0.417	1.737	1.987	-0.942	2.032	-4.78
June	5.804	0.302	2.923	1.182	1.173	-0.457	-1.78
July	73.463	0.446	2.472	0.58	1.813	0.373	0.17
August	12.798	0.238	2.461	0.226	1.36	1.46	-34.46
September	28.715	0.312	1.934	2.943	1.542	-1.682	-0.24

training data. The scatter plot of the discharge against the observed suspended sediment load and the estimated suspended sediment by ACO models of April is as shown in Figure 10. Also in Figure 11, scatter plot for the observed and estimated suspended sediment for April is drawn by parameters found as a result of ACO optimisation.

DISCUSSION

The various GA models were compared together for Nodeh station, as shown in Table 4. As seen from the table, the GA model for the current discharge and one previous discharge input combination (GA2) for most of the months (about 8 month) had the lowest RMSE and

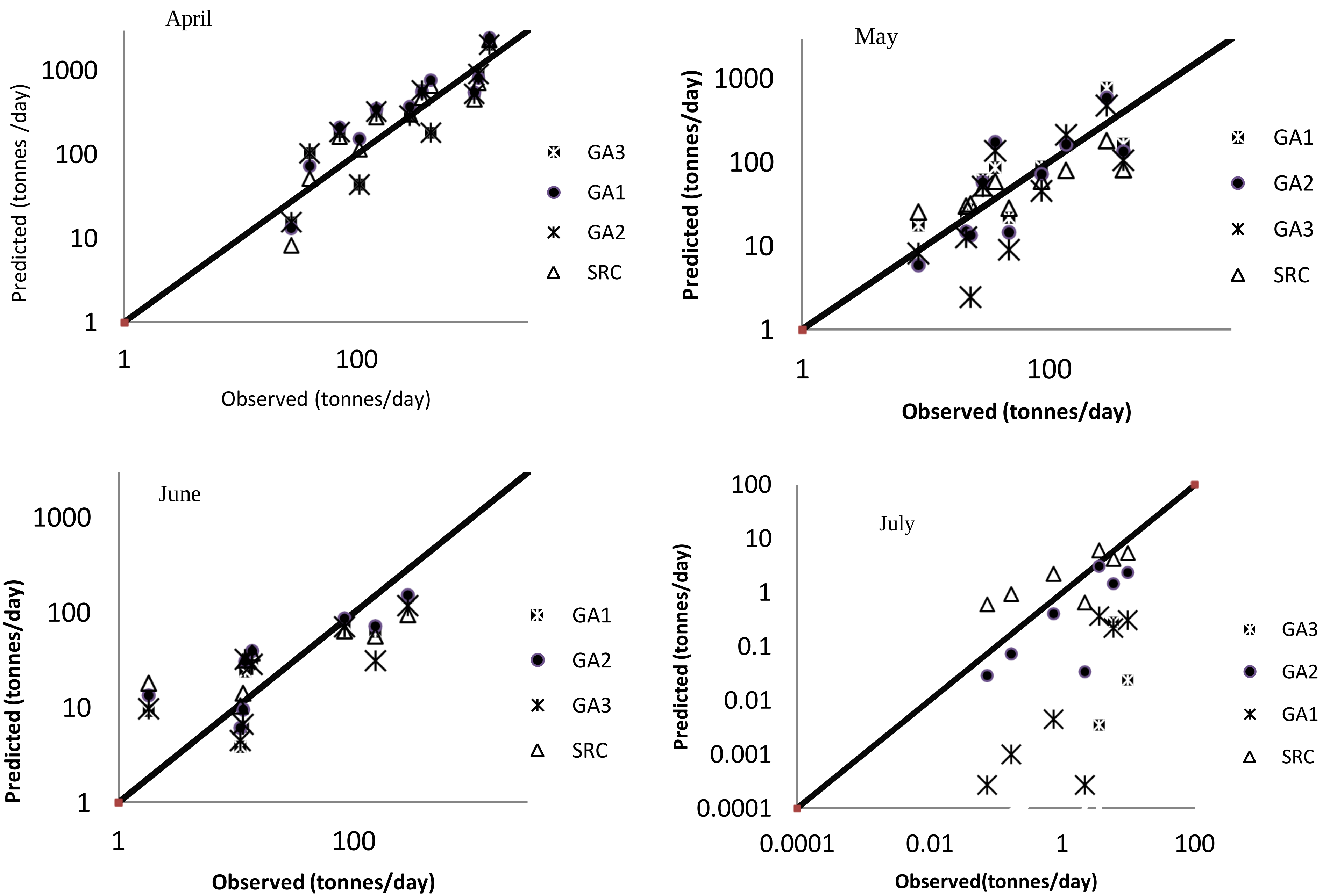
April
Predicted (tonnes /day)
1000
100
10
1
1
100
Observed (tonnes/day)
GA3
GA1
GA2
SRC
May
Predicted (tonnes/day)
1000
100
10
1
1
100
Observed (tonnes/day)
GA1
GA2
GA3
SRC
June
Predicted (tonnes/day)
1000
100
10
1
1
100
Observed (tonnes/day)
GA1
GA2
GA3
SRC
July
Predicted (tonnes/day)
100
10
1
0.1
0.01
0.001
0.0001
0.0001
0.01
1
100
Observed(tonnes/day)
GA3
GA2
GA1
SRC

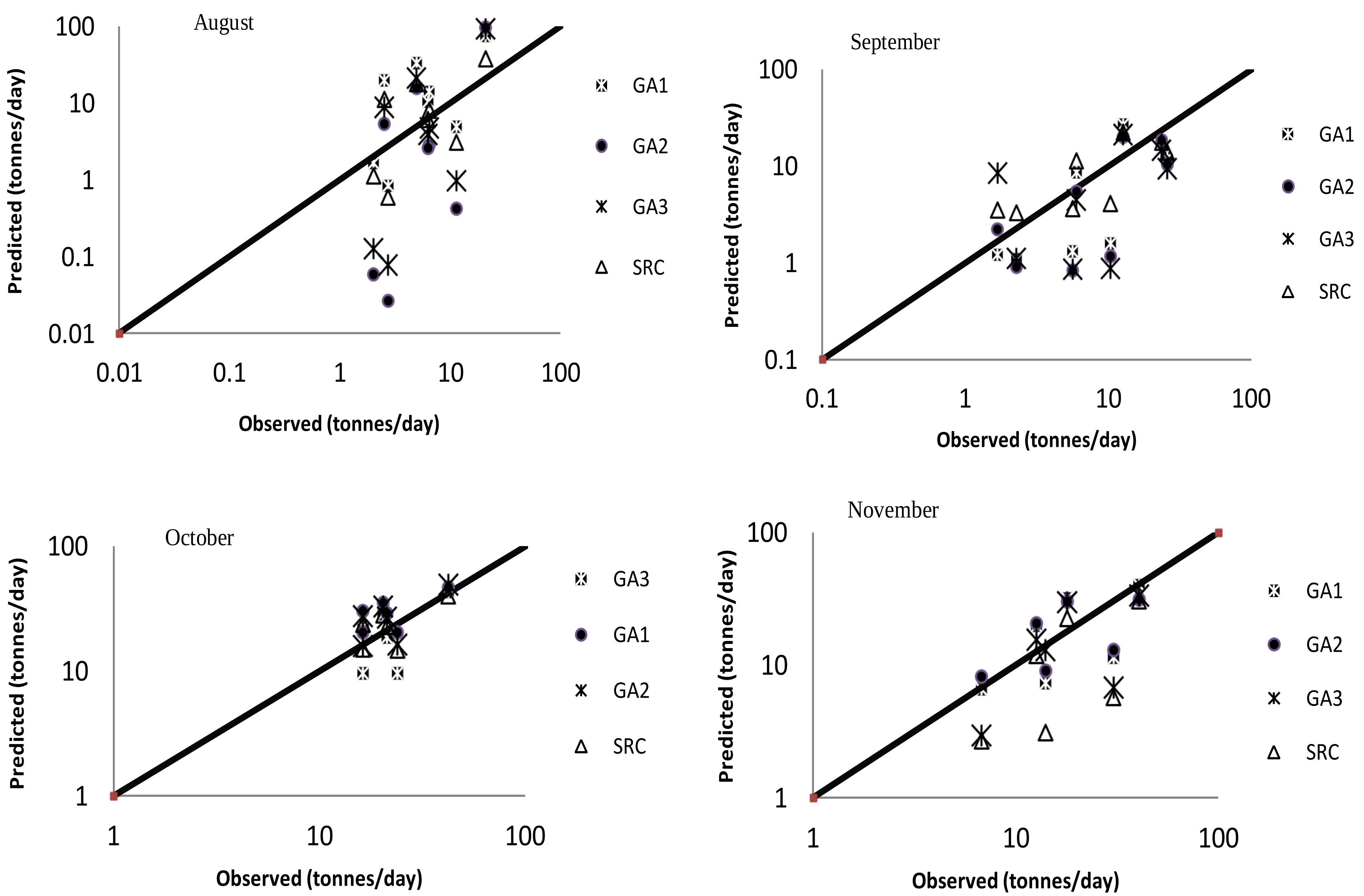
August
Predicted (tonnes/day)
Observed (tonnes/day)
100
10
1
0.1
0.01
0.01
0.1
1
10
100
GA1
GA2
GA3
SRC
September
Predicted (tonnes/day)
Observed (tonnes/day)
100
10
1
0.1
0.1
1
10
100
GA1
GA2
GA3
SRC
October
Predicted (tonnes/day)
Observed (tonnes/day)
100
10
1
1
10
100
GA3
GA1
GA2
SRC
November
Predicted (tonnes/day)
Observed (tonnes/day)
100
10
1
1
10
100
GA1
GA2
GA3
SRC

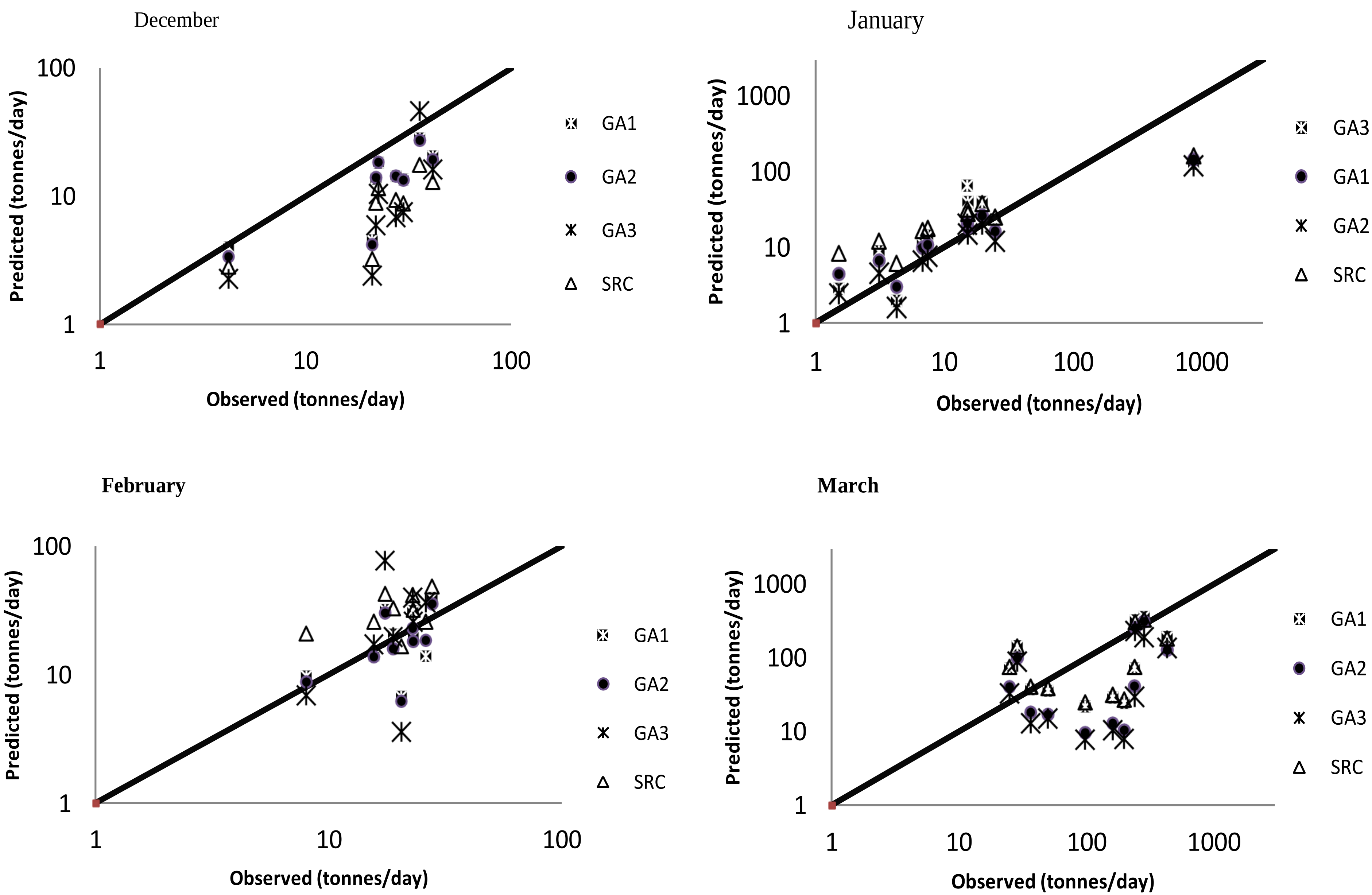

Figure 9. Scatter plot for observed and predicted suspended sediment for test period for various model of GA.

Table 5. The RMSE (ton/day), coefficient of correlation and determination coefficient of various ACO and SRC models for test period.

Test period	RMSE	R^2	a	b	c	d	CE
ACO1							
October	84.477	0.677	9.489	2.24	-	-	0.64
November	28.967	0.37	11.608	1.804	-	-	0.48
December	17.627	0.741	12.77	1.875	-	-	-1.34
January	0.821	0.426	12.665	1.222	-	-	0.69
February	1.549	0.536	5.228	2.229	-	-	0.4
March	3.59	0.372	7.236	1.894	-	-	0.29
April	3.892	0.634	11.472	1.471	-	-	-1.11
May	4.817	0.333	3.62	1.87	-	-	0.48
June	4.504	0.565	5.458	2.229	-	-	-0.16
July	57.257	0.905	7.656	1.828	-	-	0.50
August	8.047	0.042	12.34	1.23	-	-	-2.07
September	30.909	0.244	5.17	2.171	-	-	-0.23
ACO2							
October	73.117	0.748	2.241	0.962	-	-	0.73
November	50.485	0.376	7.744	2.604	-	-	-0.58
December	11.529	0.895	8.587	2.099	-	-	0.86
January	1.479	0.488	14.987	3.675	-	-	0.95
February	8.696	0.624	2.534	3.938	-	-	-16.4
March	5.482	0.432	2.885	13.92	-	-	-2.18
April	4.709	0.553	15.519	0.984	-	-	-1.16
May	4.907	0.205	3.663	1.897	-	-	-5.51
June	3.928	0.599	6.552	2.135	-	-	-0.53
July	58.382	0.693	19.345	0.987	-	-	0.48
August	7.34	0.269	10.1	0.223	-	-	-2.32
September	32.451	0.239	3.066	2.5	-	-	-0.49
ACO3							
October	90.541	0.661	0.615	1.429	1.144	1.001	0.58
November	31.804	0.114	8.8	1.421	1.919	-0.999	0.37
December	30.476	0.892	8.587	1.909	0.912	0.01	-0.37
January	6.784	0.117	30.956	0.442	4.873	0.001	-14.53
February	2.437	0.685	6.327	-0.313	2.11	0.001	-0.4
March	21.82	0.166	15.985	2.424	1.546	0.001	-49.40
April	7.112	0.55	3.041	0.896	1.994	0.001	-7.95
May	5.939	0.09	2.79	1.876	0.987	0.1	-8.54
June	4.036	0.529	5.885	-0.142	3.891	-1.999	-0.12
July	55.303	0.245	9.344	0.394	2.426	0.006	0.53
August	12.57	0.255	3.078	1.001	3.973	-1.999	-31.09
September	28.173	0.388	13.673	3.332	0.003	-1.2	0.03

the highest R^2, also, the Nash Sutcliffe efficiency (CE) for most of the month for GA2 is better from other models. In this case, for example, in April, the RMSE, R^2 and CE values for the GA1 model were 117.83, 0.68 and -0.16, respectively. On the other hand, the RMSE, R^2 and CE values for the GA2 model were 86.93, 0.74 and 0.39 and as for the GA3 model, they were 130.20, 0.63 and 0.21, correspondingly. Figure 8 shows the scatter plot of the discharge against the observed suspended sediment load and several GA model (that is, GA1, GA2 and GA3) predictions of Nodeh station. The GA performance for the first input combination of GA1 (only the current discharge) was low. For the high value of the discharge in GA2 (the current discharge and one previous discharge),

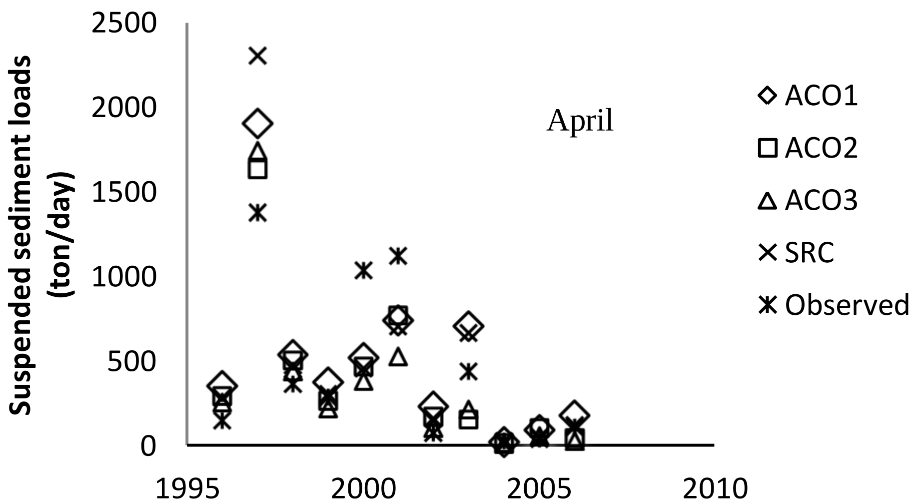

Figure 10. The scatter plot of the discharge against the observed suspended sediment load and the estimated suspended sediment by ACO models of Nodeh station during test period in April.

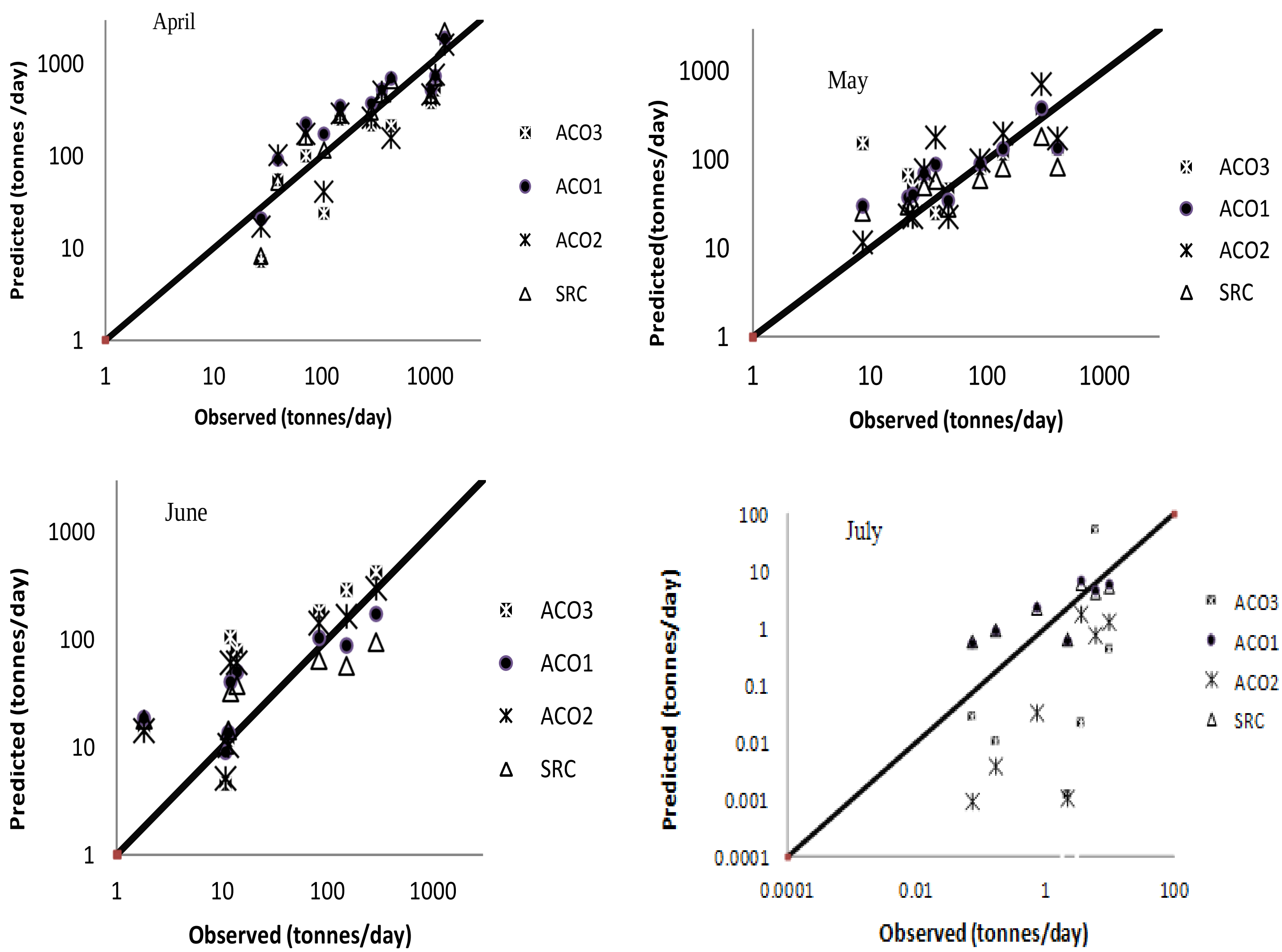

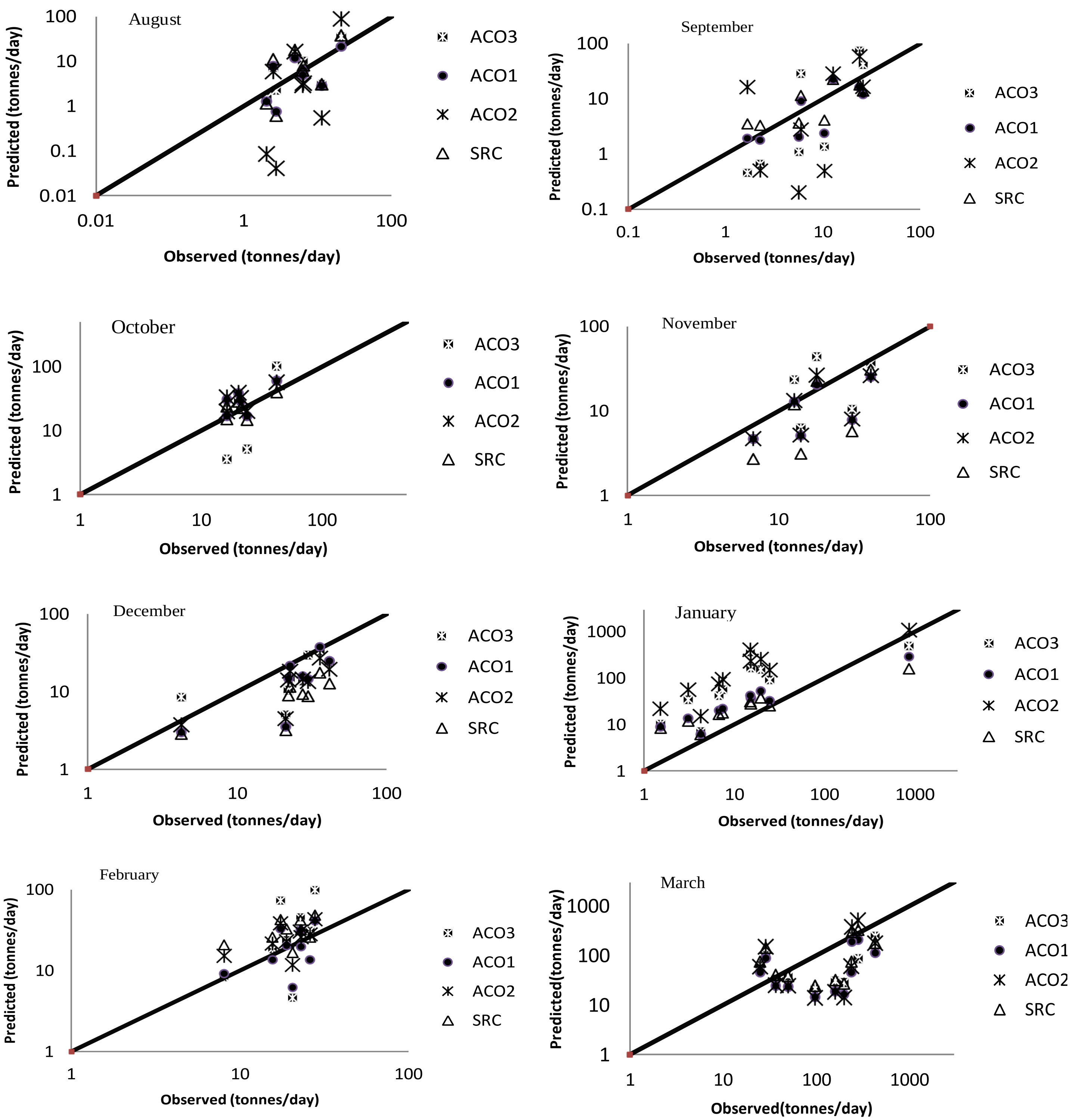

Figure 11. Scatter plot for observed and predicted suspended sediment for test period for various model of ACO.

it revealed a good performance; however, the GA3 for the peak value of the discharge had low performance.

For Nodeh station, the RMSE and the determination coefficient of various ACO models are given in Table 5. The ACO1 model provided the best accuracy for the input combination data. On the contrary, the ACO3 model with the input of the current discharge and one and two of previous discharges performed the worst model in the Nodeh station. As shown in Table 5, the ACO model with the inputs of current discharge (ACO1) for most of the

Table 6. The RMSE (ton/day), coefficient of correlation of ACO1, GA2 and SRC models for test period.

Test period	SRC			ACO1			GA2		
	RMSE	R^2	CE	RMSE	R^2	CE	RMSE	R^2	CE
April	109.447	0.656	0.54	84.477	0.677	0.62	86.926	0.736	0.64
May	34.549	0.168	-5.47	28.967	0.37	-0.15	42.998	0.347	0.48
June	27.241	0.408	-1.89	17.627	0.741	0.65	19.788	0.8	-1.34
July	0.839	0.389	0.25	0.821	0.426	-0.8	1.6784	0.595	0.69
August	3.101	0.579	-6.05	1.549	0.536	-21.6	9.899	0.619	0.4
September	3.942	0.325	0.05	3.59	0.372	0.29	2.599	0.473	0.29
October	5.539	0.525	0.39	3.892	0.634	0.09	4.557	0.599	-1.11
November	4.893	0.417	0.26	4.817	0.333	0.39	4.171	0.054	0.48
December	4.54	0.61	-0.62	4.504	0.565	-0.56	3.947	0.593	-0.16
January	69.876	0.801	0.57	57.257	0.905	0.15	74.174	0.91	0.5
February	8.522	0.065	-1.2	8.047	0.042	-0.84	7.729	0.295	-2.07
March	23.328	0.238	0.42	30.909	0.244	-0.2	27.678	0.259	-0.23

related months (about 10 month) had the lowest RMSE and the highest R^2. Also, ACO1 for 8 month has good CE from other models. In this case, for example, in May, the RMSE, R^2 and CE values for the ACO1 model were 28.97, 0.37 and 0.48, respectively. On the other hand, the RMSE, R^2 and CE for the ACO2 model were 50.48, 0.38 and -5.51, respectively, and 31.8, 0.11 and -8.58, accordingly, for the ACO3 model. Figure 10 displays the scatter plot for the observed and estimated suspended sediments for April, drawn from the various ACO optimisations. For most of the values of discharge, ACO1 and ACO2 revealed good performance, whereas ACO3 for the peak value of discharge showed low performance.

ACO1 model was compared with the GA2 and SRC models as shown in Table 6, for Nodeh station, because between the sub models of ACO and GA, ACO1 and GA2 have good performance from the other. It can be obviously seen from this table that the ACO1 model performed much better than the rating curve techniques. However, the GA2 technique had a RMSE value slightly better than the SRC model. It appeared that the accuracy of the ACO model seemed to be better than the SRC model. In addition, it can be observed from Table 6 that the performance of the ACO model was much better than the SRC and GA techniques when the input to both GA and ACO and the rating curve model was only the current discharge. Furthermore, after the ACO model, the GA model was better than SRC. In this case, for example, in May, the RMSE, R^2 and CE values for the ACO1 model were 28.97, 0.37and 0.48, respectively. On the other hand, the RMSE, R^2 and CE values for the GA2 model were 43, 0.35 and 0.39, and as for the SRC model, they were 34.5, 0.17 and 0.26, respectively. The suspended sediment estimation of ACO1, GA2 and SRC and the observed values were compared, as shown in Figure 12. As shown in the figure, the ACO1 model approximated the corresponding observed suspended sediment values better than the rating curve and GA2 techniques. The GA2 performed better than the SRC model. Apparently, the ACO1 seemed to have better accuracy than the GA2 model. Moreover, it can be seen from this figure that the ACO1 model estimation was closer to the observed suspended sediment values than the rating curve and GA2 techniques for peak value (especially the SRC).

Conclusions

Alternatively, in this study, the parameters obtained by ACO and GA produced many sets of coefficient providing a relationship between Q_w and Q_s. The study showed the ability of the ACO technique to model the relationship between the stream flow and the suspended sediment. The model provides a practical way for sediment estimation, producing accurate results and encouraging the use of ACO in other aspects of water engineering studies. The suspended sediment estimations based on the ACO models were compared with GA and sediment rating curves. For the monthly suspended sediment estimation, the results indicated that the ACO1 model provided better performance in estimating the suspended sediment loads as compared to other ACO models. Also, the GA2 model was more accurate than GA1 and GA2. It can be obviously seen from the results that the ACO1 model performed much better than the rating curve techniques. However, the GA2 technique had slightly better value of RMSE than the SRC model. The accuracy of the SRC models seemed to be better than the ACO3 model from the variety of ACO models. In addition, it can be observed from the results that the performance of the SRC model was more inferior than ACO and GA techniques when the input to both GA and ACO and the rating curve model was only the current discharge. Also, after using the ACO model, the GA model was better than SRC. As seen from the results, the ACO1 model approximated the corresponding of the observed

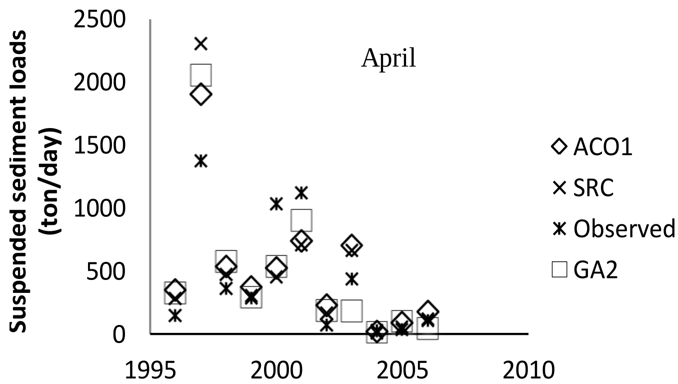

Figure 12. The scatter plot of the discharge against the observed suspended sediment load and the estimated suspended sediment by the best ACO, best GA and SRC models of Nodeh station during test period in April.

suspended sediment values better than the rating curve and GA2 techniques. The ACO1 seemed to have a better accuracy than the GA2 model. It was seen from the results that both the low and high sediment values and in general the overall shape of the sediment time series were closely approximated by the ACO1 for the monthly method. However, for the peak flow discharge, the GA2 could predict the suspended sediment better than ACO1 and SRC. From the mentioned results, it can be concluded that the suspended sediment discharge had high relationship with the current discharge and one-day previous discharge, whereas, it was an infirm relation between the two-day previous discharge and the suspended sediment discharge. There were a lot of research studies in the literature that looked at the prediction of sediment loads. However, only Altunkaynak (2009) applied the GA for suspended sediment estimation for the lower Mississippi river basin. He proposed a relationship between the sediment loads and the discharge by using GA. His results showed that GA provided better solutions than regression model (RM) with respect to the errors calculated by R^2 and mean relating error (MRE). Considering Altunkaynak (2009) research for the sediment loads, the results of this investigation were also confirmed. However, ant colony optimization is applied more in water resource engineering, such as ground water, pipe network optimization and water distribution network. Nevertheless, there is no application for surface water resource, especially in suspended sediment estimation. In addition, Abbaspour et al. (2001) used the ACO algorithm for estimating the un-saturated soil hydraulic parameters. The results obtained with the ant colony parameter optimization method were very promising, that is, in eight different applications, they were able to estimate the true parameter within a few percent.

Some of the advantages and disadvantages of the ACO algorithm and GA can be summarized as follows:

1) Optimization can be made through continuous or non-continuous variables.
2) It is possible to start searching from many different points at solution space so that through numerous variables, global optimization is possible.
3) Even in case of target functions with extreme values, optimization is possible.
4) ACO and GA produce a set of solution points during an adaptive and dynamic system structure evolution.
5) GA and ACO approaches provide the most suitable solution in the quickest way for an optimization problem. The GA and ACO solution has different facets than classic optimization methods. They seem as indefinite methods due to the random sampling procedure and rules at their basis.
6) One of the advantages of GA and ACO is its ability to generate more than one optimum solution points. On the other hand, SRC with the limiting assumptions can only estimate one solution point.

Another reason why the ACO and GA approach should be preferred is the independency of them from restrictive assumptions.

The power of GA comes from the fact that the technique is robust and can deal successfully with wide range of difficult problems. GA is not guaranteed to find the global optimum solution to a problem, but they are generally good at finding acceptably good solutions to problems acceptably quickly. Where specialized techniques exist for solving particular problems, they are likely to outperform GA in both speed and accuracy of the final result.

Disadvantages of these classical models, same ACO are that the calculations take too much time. In ACO degree of parameter, conditioning may be directly controlled through iteration. The more iteration we perform, the conditioned parameters being sought will become on the set, measured data. In general, we do not recommend obtaining highly conditioned parameters, as they will perform poorly when simulating other variables not included in the objective function. To find a global maximum, two techniques must be used for any efficient optimization algorithm: exploration to investigate new and unknown areas in the search space, and exploitation to make use of knowledge found at points previously visited to help find better points. These two requirements are contradictory, and a good search algorithm must find a trade off between the two.

REFERENCES

Abbaspour KC, Schulin R, van Genachten MTH (2001). Estimating unsaturated soil hydraulic parameters using ant colony optimization. Adv. Water Resour.. 24:827-841.
Afshar MH (2005). A new transition rule for ant colony optimisation algorithms: Application to pipe network optimisation problems. Eng. Optim. 37(5):525-540.
Altunkaynak A (2009). Sediment load prediction by genetic algorithms. J. Adv. Eng. Softw. 40:928-934.

Altunkaynak A, Wang K (2010). Triple diagram models for prediction of suspended solid concentration in Lake Okeechobee, Florida. J. Hydrol. 387(3-4):165-175.

Altunkaynak A (2010) Suspended sediment concentration prediction by Geno-Kalman filtering. Int. J. 37(12):8583-8589.

Blum C, Rol AI (2003). Metaheuristics in combinatorial optimization: Overview and conceptual comparison. ACM Comput. Surv. 35(3):268-308.

Cai X, McKinney DC, Lasdon LS (2001). Solving nonlinear water management models using a combined genetic algorithm and linear programming approach. Adv. Water Resour. 24(6):667-676.

Dorigo M (1992). Optimization, learning and natural algorithms (in Italian), Ph.D. Thesis, Dipartimento di Elettronica, Politecnico di Milano, Italy.

Dorigo M, Maniezzo V, Colorni A (1996). Ant system: optimization by a colony of cooperating agents. IEEE Trans. Syst. Man Cybernet. Part B. 26(1):29-41.

Espinoza FP, Minsker BS, Goldberg DE (2005). Adaptive hybrid genetic algorithm for groundwater remediation design. J. Water Res. Plan. Manage. 131(1):14-24.

Gambardella LM, Taillard E D, Agazzi G (1999). MACS-VRPTW: A multiple ant colony system for vehicle routing problems with time windows, In: Corne D, Dorigo M, Glover F (Eds.). New Ideas in Optimization, McGraw-Hill, London, UK pp. 63-76.

Glover F, Kochenberger G (Eds.) (2002). Handbook of Metaheuristics, Kluwer Academic Publishers, Norwell, MA.

Hilton ABC, Culver TB (2005). Remediation design under uncertainty using genetic algorithms. J. Water Res. Plan. Manage. 131(1):25-34.

Hoos HH, Stutzle T (2004). Stochastic Local Search: Foundations and Applications, Elsevier, Amsterdam, The Netherlands.

James WRC, Wan B, James W (2002). Implementation in PCSWMM using Genetic Algorithms for auto calibration and design optimization. In: Proceedings 9th International Conference on Urban Drainage, Portland, USA.

Leguizamon G, Michalewicz Z (1999). A New Version of Ant System for Subset Problems. Proceedings of the 1999 Congress on Evolutionary Computation, Washington DC, pp. 1459-1464.

Leopold LB, Wolman MG, Miller JP (1992). Fluvial Processes in Geomorphology. Freeman, San Francisco, California p. 522.

Liong SY, Chan WT, ShreeRam J (1995). Peak-flow forecasting with genetic algorithms and SWMM. J. Hydr. Eng. ASCE 121(8):613-617.

Mahinthakumar G, Sayeed M (2005). Hybrid genetic algorithm – Local search methods for solving groundwater source identification inverse problems. J. Water Res. Plan. Manage. 131(1):45-57.

Maier HR, Simpson AR, Zecchin AC, Foong WK, Phang KY, Seah HY (2003). Ant colony optimization for design of water distribution systems. J. Water Resour. Plan Manage. ASCE 129(3):200-2009.

Maniezzo V (1996). "Exact and Approximate Nondeterministic Tree-Search Procedures for the Quadratic Assignment Problem." Research Report CSR 98-1, 1998, Universita di Bologna, Italy Marshall, T.J., J.W. Holmes, and C.W. Rose. Soil Physics (Third Edition). New York, Cambridge University Press p. 453.

Mariano C, Morales E (1998). A multiple objective Ant-Q algorithm for the design of water distribution irrigation networks.

Nash JE, Sutcliffe JV (1970). River flow forecasting through conceptual models, Part I-A discussion of principles. J. Hydrol. 10:282-290.

Parker M, Savic DA, Walters GA, Kapelan Z (2000). SEWERNET: A genetic algorithm application for optimizing urban drainage systems. In: International Conference on Urban Drainage via Internet, 2000. Available from: http://www.dhi.cz/ICUDI.

Savic D, Walters G (1999). Genetic algorithms for the least-cost design of water distribution networks. J. Water Resour. Plan. Manage. ASCE 123(2).

Schoofs L, Naudts B (2000). Ant Colonies are Good at Solving Constraint Satisfaction Problems, Proceedings of the 2000 Congress on Evolutionary Computation, San Diego, CA, pp. 1190-1195.

Sen Z, Öztopal A (2001). Genetic algorithms for the classification and prediction of precipitation occurrence. Hydrol. Sci. J. 46(2):255-268.

Sen Z, Özger M (2004). Sediment concentration and its prediction by perceptron Kalman Filtering procedure. J. Hydr. Eng. 130:816.

Simpson AR, Maie HR, Foong WK, Phang KY, Seah HY, Tan CL (2001). Selection of parameters for ant colony optimization applied to the optimal design of water distribution systems. In: Proceedings in Congress on Modelling and Simulation, Canberra (Australia) pp. 1931-1936.

Stutzle T, Hoos HH (2001). MAX–MIN ant system. Fut. Gener. Comput. Syst. 16:889-914.

Zecchin AC, Maier HR, Simpson AR, Roberts A, Berrisford MJ, Leonard M (2003). Max-Min ant system applied to water distribution system optimization. Modsim 2003- International Congress on Modelling and Simulation, 14-17 July, Vol. 2. Townsville (Australia): Modelling and Simulation Society of Australia and New Zealand Inc, pp. 795-800.